Bridging the Gap Between Functional and Anatomical Features of Cortico-Cerebellar Circuits Using Meta-Analytic Connectivity Modeling

Joshua H. Balsters,[1,2] Angela R. Laird,[3] Peter T. Fox,[4,5] and Simon B. Eickhoff[6,7]*

[1]*Neural Control of Movement Lab, Department of Health Sciences and Technology, ETH Zurich, Switzerland*
[2]*Trinity College Institute of Neuroscience, Trinity College Dublin, Dublin, Ireland*
[3]*Department of Physics, Florida International University, Miami, Florida*
[4]*Research Imaging Center, University of Texas Health Science Center San Antonio, San Antonio, Texas*
[5]*South Texas Veterans Administration Medical Center, San Antonio, Texas*
[6]*Institute of Neuroscience and Medicine (INM-1), Research Center Jülich, Germany*
[7]*Institute of Clinical Neuroscience and Medical Psychology, Heinrich-Heine University Düsseldorf, Germany*

Abstract: Theories positing that the cerebellum contributes to cognitive as well as motor control are driven by two sources of information: (1) studies highlighting connections between the cerebellum and *both* prefrontal and motor territories, (2) functional neuroimaging studies demonstrating cerebellar activations evoked during the performance of both cognitive and motor tasks. However, almost no studies to date have combined these two sources of information and investigated cortico-cerebellar connectivity during task performance. Through the use of a novel neuroimaging tool (Meta-Analytic Connectivity Modelling) we demonstrate for the first time that cortico-cerebellar connectivity patterns seen in anatomical studies and resting fMRI are also present during task performance. Consistent with human and non-human primate anatomical studies cerebellar lobules Crus I and II were significantly coactivated with prefrontal and parietal cortices during task performance, whilst lobules HV, HVI, HVIIb, and HVIII were significantly coactivated with the pre- and postcentral gyrus. An analysis of the behavioral domains showed that these circuits were driven by distinct tasks. Prefrontal-parietal-cerebellar circuits were more active during cognitive and emotion tasks whilst motor-cerebellar circuits were more active during action execution tasks. These results highlight the separation of prefrontal and motor cortico-cerebellar loops during task performance, and further demonstrate that activity within these circuits relates to distinct functions. *Hum Brain Mapp 00:000–000, 2013.*

Key words: cerebellum; meta-analytic connectivity modeling; cognition

Additional Supporting Information may be found in the online version of this article.

*Correspondence to: Simon B. Eickhoff, Institut für Neurowissenschaften und Medizin (INM-1), Forschungszentrum Jülich GmbH, D-52425 Jülich, Germany. E-mail: S.Eickhoff@fz-juelich.de

Received for publication 8 February 2013; Revised 29 July 2013; Accepted 31 July 2013.

DOI 10.1002/hbm.22392

Published online 00 Month 2013 in Wiley Online Library (wileyonlinelibrary.com).

INTRODUCTION

A number of authors have suggested that in order to understand the functional properties of a brain region one must understand its anatomical features and connections [Crick and Koch, 2005; Eickhoff and Grefkes, 2011; Passingham et al., 2002]. A great deal is known about the intrinsic microstructure of the cerebellum [Eccles et al., 1967], and a large number of studies have mapped cortico-pontine and cortico-cerebellar connections in humans and non-human primates [see Ramnani, 2011; Strick et al., 2009 for review]. Theories of cortico-cerebellar information processing have been in a large part driven by our understanding of cortico-cerebellar connectivity. Studies in both humans [Buckner et al., 2011; Habas et al., 2009; Krienen and Buckner, 2009; O'Reilly et al., 2010; Ramnani et al., 2006] and non-human primates [Kelly and Strick, 2003; Middleton and Strick, 2000, 2001; Schmahmann and Pandya, 1997] have repeatedly demonstrated that the cerebellum receives inputs from a wide range of cortical territories including (but not restricted to) the premotor and primary motor cortices, medial and dorsal prefrontal cortex, and parietal cortex. Studies in nonhuman primates have also suggested that prefrontal and motor cortico-cerebellar circuits are completely independent of one another and do not exchange information at any point within the loop except for within the frontal lobe. Kelly and Strick [2003] showed in non-human primates that the arm area of the primary motor cortex projected to cerebellar lobules HV, HVI, HVIIb, and HVIII, whilst tracer label injected into the dorsal bank of the sulcus principalis (putatively Walker's Area 46) terminated in cerebellar lobules Crus I and Crus II. These same connections have been shown in humans using resting state fMRI [Buckner et al., 2011; Habas et al., 2009; Krienen and Buckner, 2009; O'Reilly et al., 2010]. Given that the cerebellum receives inputs from prefrontal and parietal regions that are known to process abstract information [Badre and D'Esposito, 2009], and that this information does not integrate with motor cortico-cerebellar circuits, it would suggest that the cerebellum is not solely processing motor information. However, in order to further develop theories of cortico-cerebellar connectivity it is necessary to corroborate these findings with task-based information.

Along with studies of anatomical and functional connectivity, task-based functional neuroimaging studies have provided a wealth of evidence suggesting that the cerebellum is involved in processing both motor and non-motor information [see Stoodley, 2012 for review]. Petacchi et al., [2005], Moulton et al. [2010], and Stoodley and Schmahmann [2009] have all conducted meta-analyses investigating task-dependent cerebellar processing. Whilst Petacchi et al. [2005] and Moulton et al., [2010] focused on auditory and pain processing respectively, Stoodley and Schmahmann [2009] investigated cerebellar processing during a variety of tasks ranging from cognitive to motor to emotion. They found that cerebellar lobules Crus I and II were active in studies investigating executive function, working memory, and language tasks, whilst motor control tasks consistently activated cerebellar lobules HV, HVI, and HVIII. This work thus provides further evidence that distinct regions of the cerebellum process distinct forms of information, both motor and associative. Although these findings are in keeping with cortico-cerebellar anatomy (i.e., cerebellar lobules interconnected with prefrontal cortex are active during associative tasks) it is essential to investigate cortico-cerebellar connectivity during task performance in order to ascertain the roles of cortico-cerebellar circuits in cognitive and motor control.

This study uses a novel neuroimaging tool [Meta-Analytic Connectivity Modelling (MACM)] to integrate connectivity information with behavioral information and as such extend our understanding of cortico-cerebellar information processing. MACM assesses brain-wise co-activation patterns of an anatomical region across a large number of databased neuroimaging results [Eickhoff et al., 2011; Laird et al., 2009a]. First, we identified for each voxel of the seed VOI those experiments in the BrainMap database that reported activation at that particular location. By performing an Activation Likelihood Estimation (ALE) meta-analysis over these experiments, we can generate a whole brain activation map showing all the brain regions that are active when voxels in the seed VOI are active. Differences in the coactivation patterns of the respective VOIs can be tested by directly contrasting the regional MACM patterns. Finally, in order to confirm a functional separation between the anatomical VOIs selected in this study we can assess the behavioral domain and paradigm class meta-data of experiments associated with the ensuing clusters. This manuscript describes the application of MACM to cortico-cerebellar connectivity and the ensuing behavioral differences.

METHODS

Cerebellar VOIs

Cerebellar lobules of interest were selected based on previous studies of primate cortico-cerebellar connectivity, specifically Kelly and Strick [2003]. Kelly and Strick [2003] is the only study performed on non-human primates that traced anatomical connections from regions of the frontal lobe (dorsal bank of the sulcus principalis (Walker's Area 46; Walker, 1940) and the hand/arm region of the primary motor cortex) all the way to the cerebellar cortex. We decided to restrict our analyses to cerebellar lobules found in Kelly and Strick [2003], namely vermal and hemispheric lobules V, VI, Crus I, Crus II, VIIb, VIIIa and HVIIIb (accounting for 86.34% of the cerebellar cortex; Diedrichsen et al., 2009). There are also additional practical reasons to restrict our analyses to these lobules. For example, many fMRI studies do not include the very posterior

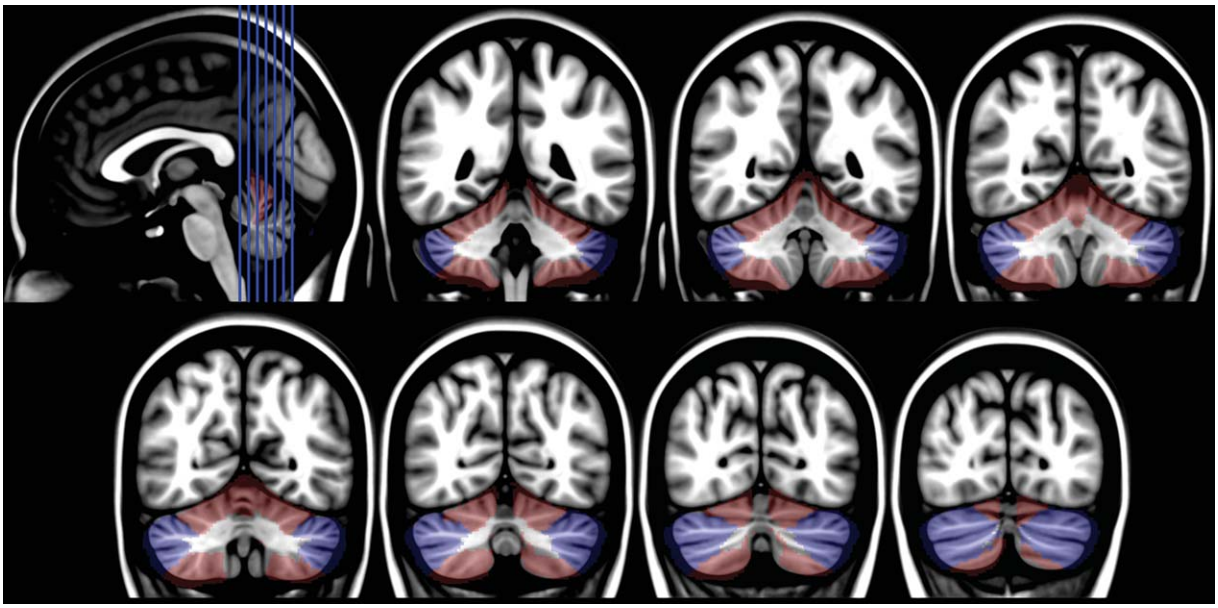

Figure 1.
Cerebellar lobular masks. Red lobules are classified as "motor" lobules (V, VI, VIIb, and VIII), blue lobules are classified as "prefrontal" lobules (Crus I and Crus II). Masks are overlayed on the FSL standard template moving from anterior-> posterior.

lobules of the cerebellum in the field of view, thus there are fewer studies reporting activations within lobules IX and X. Anterior lobules I-IV can also be contaminated by non-cerebellar signal originating from the occipital lobes directly above them, i.e., the ventral visual cortex [Diedrichsen, 2006]. Cerebellar lobular masks were extracted from the probabilistic cerebellar atlas of Diedrichsen et al. [2009] and combined to create masks of interest (see Fig. 1). For example, the seed mask for the analysis of cerebellar "motor" lobules was created by combining masks of cerebellar lobules V, VI, VIIb, and VIII (red in Fig. 1). The atlas of Diedrichsen et al. [2009] conforms to the anatomical landmarks outlined by Larsell and Jansen [1972]. Using these cerebellar lobules as seeds we investigated differences in task-based connectivity between motor-projecting cerebellar lobules (V, VI, VIIb, VIII) and prefrontal-projecting cerebellar lobules (Crus I and II). We will additionally investigate differences in task-based connectivity between anterior motor-projecting cerebellar lobules (V, VI) and posterior motor-projecting cerebellar lobules (VIIb, VIII), given that posterior motor-projecting cerebellar lobules have selectively expanded in humans compared to nonhuman primates [Balsters et al., 2010].

Meta-Analytic Connectivity Modeling

The BrainMap database [www.brainmap.org; Fox and Lancaster, 2002; Laird et al., 2005, 2009a, 2011] was employed for the retrieval of relevant neuroimaging experiments. At the time of assessment, the database contained coordinates of reported activation foci and associated meta-data of over 11,000 neuroimaging experiments. For our analysis, only whole brain studies of healthy subjects reporting activation in standard stereotaxic space were considered, while all experiments that investigated age, gender, handedness, training effects or involved a clinical population were excluded. As the first step of the analysis we identified (separately for each seed region) all experiments that featured at least one focus of activation within the respective seed (MNI space). In order to facilitate such filtering, coordinates from Talairach space were converted into MNI coordinates by using Lancaster transformation [Lancaster et al., 2007]. Then, all experiments activating the currently considered seed were identified. The retrieval was solely based on reported activation coordinates, not on any anatomical or functional label.

Functional connectivity of the different seeds was evaluated using meta-analytic connectivity modelling [MACM; Robinson et al., 2012, 2010]. The key idea behind MACM is to assess which brain regions are coactivated above chance with a particular seed region in functional neuroimaging experiments [Eickhoff et al., 2010; Laird et al., 2009b]. MACM entails to first identify all experiments in a database that activate a particular brain region as described above and then test for convergence across (all) foci reported in these experiments. Obviously, as experiments were selected by activation in the seed, highest

convergence will be observed in the seed region. Significant convergence of the reported foci in other brain regions, however, indicates consistent coactivation, i.e., functional connectivity with the seed. The whole brain peak coordinates of the identified experiments were downloaded from BrainMap database for each seed region. Coordinates were analysed with the modified activation likelihood estimation (ALE) algorithm [Eickhoff et al., 2009, 2012] to detect areas of convergence. This approach models each focus as a Gaussian distribution reflecting empirical estimates of the uncertainty of different spatial normalization techniques and intersubject variability as a function of the number of subjects. Modeled activation (MA) maps are calculated for each experiment by combining the Gaussian distributions of the reported foci [Turkeltaub et al., 2012]. Taking the union across these yielded voxel-wise ALE scores that describe the convergence of results at each particular location of the brain. To distinguish "true" convergence between studies from random convergence, i.e., noise, in the proposed revision of the ALE algorithm [Eickhoff et al., 2012], ALE scores are compared to an empirical null-distribution reflecting a random spatial association between experiments [Eickhoff et al., 2012; Turkeltaub et al., 2012]. The p-value of an observed ALE is then given by the proportion of this null-distribution (precisely, its cumulative density function) corresponding equal or higher ALE values. The ALE maps reflecting the convergence of coactivations with any particular seed region were subsequently thresholded at $P < 0.05$ cluster-level corrected (cluster-forming threshold: $P < 0.001$ at voxel-level) and converted into Z-scores for display.

For further investigation of commonalities and distinctions between the functional connectivity of different seeds, conjunction and difference analyses were performed. For conjunction analysis the minimum statistic [Nichols et al., 2005] was used, yielding voxels that showed significant values in both coactivation maps. The result corresponds to the intersection of the (cluster-level corrected) MACM maps [Caspers et al., 2010]. Difference maps were established by calculating the voxel-wise differences of the Z-scores obtained from the ALE maps of the two MACM analyses. When calculating difference maps, activation foci common to both conditions were removed. The difference maps were then tested against an ALE difference map assuming the null-distribution, which was generated from a random bipartition of the pooled experiments underlying either of the two inspected maps, at $P < 0.001$ [Eickhoff et al., 2011; Rottschy et al., 2012]. To avoid obtaining significant coactivation in voxels of the difference map that do not show significant coactivation on the underlying ALE map, the resulting maps were masked with the main effect of the respective ALE map. Furthermore, only regions with at least 20 cohesive voxels were considered in the resulting difference maps. Finally, anatomical allocation of all results was performed using the SPM Anatomy Toolbox [http://www.fz-juelich.de/inm/inm-1/spm_anatomy_toolbox, Eickhoff et al., 2005, 2006, 2007].

Functional Characterization

The functional characterization of the cerebellar regions was based on the "Behavioral Domain" and "Paradigm Class" meta-data categories available for each neuroimaging experiment included in the BrainMap database. Behavioral domains include the main categories cognition, action, perception, emotion, and interoception, as well as their related sub-categories. Paradigm classes categorize the specific task employed [see http://brainmap.org/scribe/ for the complete BrainMap taxonomy; Fox et al., 2005].

In a first step, we determined the individual functional profile of each region of interest by using the probability of a psychological process being present given knowledge of activation in a particular brain region. This likelihood P(Task|Activation) can be derived from P(Activation|Task) as well as P(Task) and P(Activation) using Bayes rule. Significance (at $P < 0.05$, corrected for multiple comparisons using Bonferroni's method) was then assessed by means of a chi-squared test [Eickhoff et al., 2011; Laird et al., 2009b; Nickl-Jockschat et al., 2011]. Second, we contrasted the functional profiles of the different regions of interest with each other. For these comparisons, the analysis was constrained to all BrainMap experiments activating either region. From this pool of experiments, the baserate is the apriori probability of any focus to lie in either of the two compared regions [Cieslik et al., 2012]. We then compared the occurrence probabilities of the tasks given activation in the one region (rather than in the other cluster) and assessed them by means of a chi-squared test ($P < 0.05$, corrected for multiple comparisons using Bonferroni's method).

RESULTS

Studies in humans [Buckner et al., 2011; Krienen and Buckner, 2009; O'Reilly et al., 2010] and nonhuman primates [Kelly and Strick, 2003] have shown that cerebellar lobules HV, HVI, HVIIb, and HVIII receive inputs from primary motor cortex, while cerebellar lobules Crus I and Crus II receive inputs from prefrontal and parietal cortices. We begin by establishing whether these connectivity patterns also exist in task-dependent data. The results below are created using masks that are the combination of these cerebellar lobules; however, MACM results for individual cerebellar lobules are available in Supporting Information. Results were calculated from the BrainMap database 24th May 2013.

Connectivity of "Motor" Lobules

Table I lists regions coactivated with cerebellar lobules HV, HVI, HVIIb, HVIII. The BrainMap database contained

TABLE I. MACM functional connectivity for lobules HV, HVI, HVIIb, and HVIII

Label	Cluster Size	Z	Co-ordinate (x y z)			Cytoarchitectonic BA (Probability if available)
Cerebellum						
Right Cerebellum	7690	9.14	22	−56	−22	Lobule VI (95%)
Left Cerebellum	same cluster	8.92	−28	−60	−26	Lobule VI (96%)
Cerebellar Vermis	same cluster	8.82	6	−64	−18	Lobule VI (59%)
Frontal Lobe						
Left Insula Lobe	7716	8.86	−34	20	2	Area 6 (60%)
Left Precentral Gyrus	same cluster	8.77	−36	−18	58	Area 6 (70%)
Left Precentral Gyrus	same cluster	8.77	−50	−6	44	Area 44 (40%)
Left Precentral Gyrus	same cluster	8.75	−48	6	32	
Left Superior Frontal Gyrus	same cluster	8.75	−26	−4	60	
Left Inferior Frontal Gyrus (p. Opercularis)	same cluster	8.59	−52	12	0	
Right Insula Lobe	2873	8.83	34	20	2	
Right Middle Frontal Gyrus	same cluster	8.64	28	−4	56	
Right Inferior Frontal Gyrus (p. Opercularis)	same cluster	8.61	52	12	26	Area 44 (40%)
RightPrecentral Gyrus	same cluster	8.61	52	−2	40	Area 6 (70%)
Left SMA	2752	9.12	−2	6	54	Area 6 (60%)
Right Middle Frontal Gyrus	163	8.01	40	40	26	
Right Precentral Gyrus	78	7.57	38	−18	60	Area 6 (80%)
Parietal Lobe						
Left Inferior Parietal Lobule	7716 (previous cluster)	8.72	−30	−56	52	SPL (7A) (40%)
Left SupraMarginal Gyrus	same cluster	8.63	−54	−24	18	OP 1 (80%)
Left Inferior Parietal Lobule	same cluster	8.58	−42	−40	42	hIP3 (20%)
Right Inferior Parietal Lobule	595	8.59	42	−44	46	hIP2 (50%)
Right Superior Parietal Lobule	same cluster	8.57	32	−56	48	hIP3 (50%)
Temporal Lobe						
Right Superior Temporal Gyrus	76	6.03	56	−24	4	
Right Middle Temporal Gyrus	same cluster	5.82	56	−36	6	
Right Superior Temporal Gyrus	62	6.2	60	−32	22	IPC (PF) (50%)
Occipital Lobe						
Left Middle Occipital Gyrus	96	7.86	−28	−92	−2	
Right Inferior Occipital Gyrus	62	6.26	32	−88	−8	hOC3v (V3v) (30%)
Left Calcarine Gyrus	38	6.13	−12	−92	−2	Area 17 (60%)
Subcortical						
Left Putamen	7716 (previous cluster)	8.8	−24	−4	4	n/a
Left Pallidum	same cluster	8.6	−18	−2	0	n/a
Right Pallidum	2873 (previous cluster)	8.73	24	2	2	n/a
Left Thalamus	1590	9.05	−12	−18	6	Th-Prefrontal (82%)
Right Thalamus	same cluster	8.87	12	−16	6	Th-Prefrontal (84%)
Left Thalamus	same cluster	8.08	−20	−16	0	Th-Premotor (32%)

Cluster size indicates the number of voxels. Cytoarchitectonic and anatomical probabilities were established where possible using the Anatomy toolbox (Eickhoff et al., 2007; Eickhoff et al., 2006; Eickhoff et al., 2005).

1,359 experiments (17,778 subjects and 19,988 foci) which fell within any of the above mentioned cerebellar lobules. The MACM analysis found that regions that covaried significantly with cerebellar "motor" lobules included bilateral precentral and postcentral gyrus (areas 4 and 6), bilateral inferior frontal gyrus (pars opercularis; area 44), Supplementary Motor Area (SMA), bilateral inferior parietal lobule (hIP3), and subcortical structures including the left putamen, the right pallidum, and bilateral thalamus (see Fig. 2a).

Connectivity of "Prefrontal" Lobules

Table II lists regions coactivated with cerebellar lobules Crus I and Crus II. The BrainMap database contained 809 experiments (10,683 subjects and 13,109 foci) which fell within any of the above mentioned cerebellar lobules. A number of regions within the prefrontal cortex were coactivated with activity in these cerebellar lobules. This included activity in the middle and inferior frontal gyrus, precentral gyrus (area 6), superior medial gyrus (Pre-SMA)

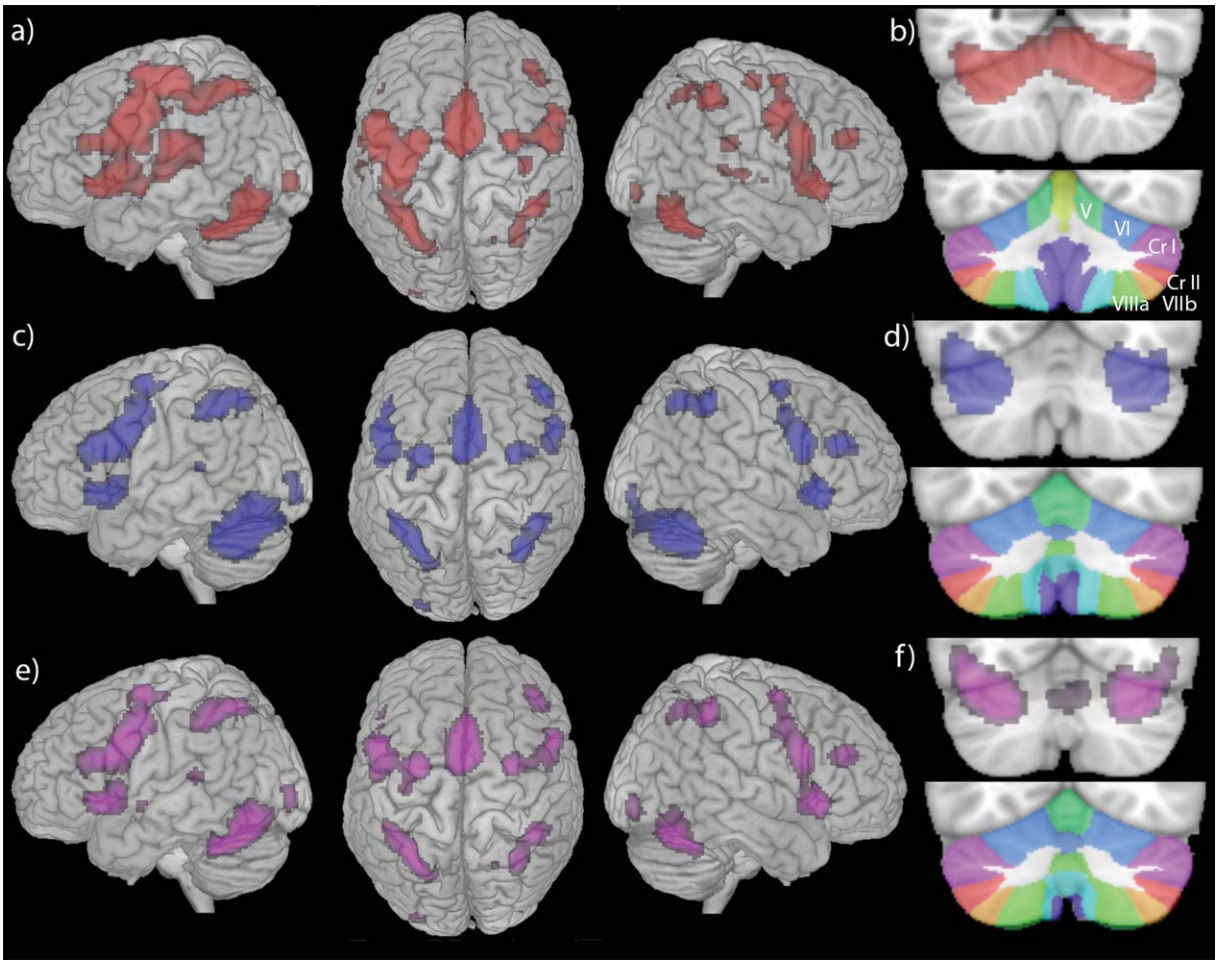

Figure 2.

MACM connectivity maps for lobules HV, HVI, HVIIb, HVIII (red, a-b), Crus I and II (blue, c-d) and overlap (purple, e-f). A, C, and E show left hemisphere, top view and right hemisphere activations rendered on ch2better.nii anatomical image. B, D, and F show coronal slices with cerebellar activations along with the same slice of the probabilistic cerebellar atlas (Diedrichsen et al., 2009) for comparison.

and bilateral insula, bilateral inferior parietal lobule, bilateral pallidum, and bilateral prefrontal-projecting regions of the thalamus (see Fig. 2c).

Common Connectivity Between "Motor" and "Prefrontal" Lobules

Table III lists regions coactivated for both "motor" lobules (HV, HVI, HVIIb, HVIII) and "prefrontal" lobules (Crus I and Crus II) as inferred from the conjunction analyses of the two respective MACMs. This analysis revealed a number of regions in the frontal lobe including inferior, middle, and superior frontal gyrus, precentral gyrus (Areas 44 and 6) and SMA. Bilateral inferior parietal lobule, right superior parietal lobule, and left superior temporal gyrus were also activated. Right pallidum and left putamen, along with bilateral thalamus (Prefrontal projecting) were also active (see Fig. 2e).

Connectivity of "Motor" vs. "Prefrontal" Lobules

Table IV lists coactivation differences between cerebellar lobules Crus I and Crus II and cerebellar lobules HV, HVI, HVIIb, HVIII. These differences are also illustrated in Figure 3. Motor lobules showed greater coactivation with motor regions within the frontal lobe (precentral gyrus and SMA; area 6), along with premotor-projecting regions of the thalamus. There was also greater connectivity with somatosensory regions (areas 1, 2, 3a, 3b), bilateral superior and medial parietal regions, bilateral superior temporal gyrus, and bilateral putamen and pallidum. Prefrontal

TABLE II. MACM functional connectivity for lobules Crus I and II

Label	Cluster Size	Z	Co-ordinate (x y z)			Cytoarchitectonic BA (Probability if available)
Cerebellum						
Left Cerebellum	3128	8.74	−32	−62	−28	Lobule VIIa Crus I (62%)
Right Cerebellum	2928	8.79	34	−64	−28	Lobule VIIa Crus I (62%)
Right Cerebellum	same cluster	8.56	26	−58	−20	Lobule HVI (78%)
Frontal Lobe						
Left SMA	2100	8.82	−2	14	48	Area 6 (30%)
Left Precentral Gyrus	1589	8.61	−48	8	30	Area 44 (30%)
Left Precentral Gyrus	same cluster	7.73	−50	−4	44	Area 6 (60%)
Left Insula Lobe	1395	8.78	−32	22	0	
Left Inferior Frontal Gyrus (p. Orbitalis)	same cluster	8.49	−48	16	−6	
Right Insula Lobe	861	8.73	38	22	−4	
Right Inferior Frontal Gyrus (p. Opercularis)	646	8.57	50	10	28	Area 44 (40%)
RightPrecentral Gyrus	same cluster	6.55	52	2	44	Area 6 (50%)
Left Superior Frontal Gyrus	341	8.6	−26	−4	62	
Left Precentral Gyrus	same cluster	6.03	−34	−16	60	Area 6 (90%)
Right Inferior Frontal Gyrus (p. Triangularis)	253	8.49	44	36	26	
Right Middle Frontal Gyrus	217	8.53	28	−4	56	
Parietal Lobe						
Left Inferior Parietal Lobule	970	8.57	−30	−56	50	SPL (7A) (50%)
Left Inferior Parietal Lobule	same cluster	8.52	−40	−48	44	hIP1 (50%)
Right Angular Gyrus	615	8.51	32	−60	50	hIP3 (40%)
Right Inferior Parietal Lobule	same cluster	8.47	42	−44	48	hIP2 (50%)
Temporal Lobe						
Left Superior Temporal Gyrus	16	5.78	−58	−38	12	
Occipital Lobe						
Left Inferior Occipital Gyrus	187	6.9	−24	−94	−4	hOC3v (V3v) (40%)
Left Middle Occipital Gyrus	same cluster	6.58	−30	−92	4	
Left Middle Occipital Gyrus	same cluster	6.52	−28	−94	2	
Subcortical						
Left Putamen	1395 (previous cluster)	8.51	−22	0	4	n/a
Left Pallidum	same cluster	6.25	−16	0	2	n/a
Left Thalamus	834	8.6	−10	−18	6	Th-Prefrontal (90%)
Right Thalamus	same cluster	8.58	10	−16	6	Th-Prefrontal (88%)
Right Pallidum	233	8.5	20	4	4	
Right Caudate Nucleus	same cluster	6.28	14	8	6	

Cluster size indicates the number of voxels. Cytoarchitectonic and anatomical probabilities were established where possible using the Anatomy toolbox (Eickhoff et al., 2007; Eickhoff et al., 2006; Eickhoff et al., 2005).

lobules showed greater coactivation with anterior regions of the frontal lobe (bilateral inferior and middle frontal gyrus [areas 44, and 45)], Pre-SMA, inferior and superior parietal lobule, and angular gyrus.

Connectivity of Anterior vs. Posterior "Motor" Lobules

Balsters et al. [2010] previously demonstrated differences in the evolutionary expansion of posterior cerebellar "motor" lobules (HVIIb and HVIII) compared to anterior cerebellar "motor" lobules (HV and HVI). We therefore used MACM to investigate task-dependent connectivity differences between these sets of cerebellar lobules. The BrainMap database contained 1,337 experiments (17,414 subjects and 19,752 foci) which fell within anterior cerebellar "motor" lobules and 202 experiments (2,477 subjects and 3,932 foci) which fell within posterior cerebellar "motor" lobules. Table V lists coactivation differences between cerebellar lobules HV, HVI and HVIIb, HVIII. These differences are also illustrated in Figure 4. Lobules HV and HVI showed greater coactivation with bilateral precentral gyrus (Area 6) and SMA, bilateral postcentral gyrus (Areas 3a,b), left superior temporal gyrus, right supramarginal gyrus, bilateral thalamus (prefrontal,

TABLE III. Conjunction between MACM functional connectivity maps for lobules HV, HVI, HVIIb, HVIII, and Crus I, II

Label	Cluster Size	Z	Co-ordinate (x y z)			Cytoarchitectonic BA (Probability if available)
Cerebellum						
Right Cerebellum	6992	8.79	34	−64	−28	Lobule VIIa Crus I (62%)
Left Cerebellum	same cluster	8.74	−32	−62	−28	Lobule VIIa Crus I (62%)
Right Cerebellum	same cluster	8.56	26	−58	−20	Lobule HVI (78%)
Left Cerebellum	same cluster	6.94	−10	−76	−26	Lobule HVI (58%)
Frontal Lobe						
Left Insula Lobe	10904	8.78	−32	22	0	
Right Insula Lobe	same cluster	8.73	38	22	−4	
Left Precentral Gyrus	same cluster	8.61	−48	8	30	Area 44 (40%)
Left Superior Frontal Gyrus	same cluster	8.6	−26	−4	62	
Right Inferior Frontal Gyrus (p. Opercularis)	same cluster	8.57	50	10	28	Area 44 (40%)
Right Middle Frontal Gyrus	same cluster	8.53	28	−4	56	
Left SMA	2729	8.82	−2	14	48	
Right Middle Frontal Gyrus	379	7.99	42	38	26	
Parietal Lobe						
Left Inferior Parietal Lobule	1444	8.57	−30	−56	50	SPL (7A)
Left Inferior Parietal Lobule	same cluster	8.51	−40	−44	44	hIP2 (30%)
Right Angular Gyrus	1087	8.5	32	−58	50	hIP3(30%)
Right Inferior Parietal Lobule	same cluster	8.47	42	−44	48	hIP2 (50%)
Right Superior Parietal Lobule	same cluster	4.98	18	−62	62	SPL (7A) (30%)
Right Superior Parietal Lobule	same cluster	3.97	16	−68	54	SPL (7P) (60%)
Temporal Lobe						
Left Superior Temporal Gyrus	231	5.66	−58	−36	12	
Left Superior Temporal Gyrus	same cluster	3.91	−58	−20	2	
Subcortical						
Left Thalamus	10904 (previous cluster)	8.6	−10	−18	6	Th−Prefrontal (88%)
Right Thalamus	same cluster	8.58	10	−16	6	Th−Prefrontal (90%)
Left Putamen	same cluster	8.51	−22	0	4	n/a
Right Pallidum	same cluster	8.5	20	4	4	n/a

Cluster size indicates the number of voxels. Cytoarchitectonic and anatomical probabilities were established where possible using the Anatomy toolbox (Eickhoff et al., 2007; Eickhoff et al., 2006; Eickhoff et al., 2005).

premotor, and motor regions), left putamen and right pallidum. Lobules HVIIb and HVIII showed greater coactivation with anterior regions of the superior medial gyrus (putatively pre-SMA), bilateral inferior frontal gyrus, left thalamus (prefrontal and parietal projecting), and right pallidum.

Behavioral Domains and Paradigm Classes for Cerebellar Lobules

Figure 5 shows the behavioral domains and paradigm classes associated with activations that fell within cerebellar lobules HV, HVI, HVIIb, and HVIII (Fig. 5a) or Crus I and II (Fig. 5b) compared with base rate (i.e., the general probability of finding BrainMap activation in the seed), and the differences between these sources (Fig. 5c). As expected, studies activating cerebellar lobules HV, HVI, HVIIb, and HVIII were typically motor tasks, specifically action execution (see Fig. 5a). Studies where participants performed overt reading, flexion and extension, drawing and finger tapping activated cerebellar motor lobules greater than chance (Fig. 5a). In contrast, studies involving working memory and pain perception activated cerebellar lobules Crus I and II (Fig. 5b green). Drawing and the Stroop task activated these lobules greater than chance. When comparing these two masks ("motor" vs. "prefrontal" cerebellar lobules) we see that motor lobules were active during action execution compared with prefrontal lobules (Fig. 5c red) whereas attention, working memory and emotion activated "prefrontal" lobules compared with "motor" lobules (Fig. 5c green). Reading and finger tapping paradigms significantly activated "motor" lobules compared to "prefrontal" lobules whereas the Simon task, Stroop task and passive listening all significantly activated "prefrontal" lobules compares to "motor" lobules (Fig. 5c green).

TABLE IV. Differences in MACM functional connectivity between lobules HV, HVI, HVIIb, HVIII and Crus I, II

Motor > PFC Label	Cluster Size	*Z*	Co-ordinate (*x y z*)			Cytoarchitectonic BA (Probability if available)
Cerebellum						
Rigth Cerebellum	7037	8.13	24	−58	−34	Lobule HVI (18%)
Frontal Lobe						
Left Insula Lobe	6841	5.11	−40	−2	2	
Right Insula Lobe	2454	5.01	36	4	6	
Left Middle Cingulate Cortex	1632	8.13	−2	2	40	
Left SMA	same cluster	3.94	−8	−4	64	Area 6 (50%)
Right Precentral Gyrus	289	7.57	38	−18	60	Area 6 (80%)
Right Middle Cingulate Cortex	78	3.22	6	14	32	
Parietal Lobe						
Left Rolandic Operculum	6841 (previous cluster)	7.18	−48	0	6	
Left Postcentral Gyrus	same cluster	5.08	−34	−36	46	SPL (7PC) (20%)
Left Inferior Parietal Lobule	same cluster	4.42	−52	−22	38	Area 2 (70%)
Left Inferior Parietal Lobule	same cluster	3.8	−50	−28	36	IPC (PFt) (60%)
Right Postcentral Gyrus	2454 (previous cluster)	7.28	56	−4	34	Area 6 (50%)
Right Postcentral Gyrus	same cluster	4.28	58	0	18	Area 3b (30%)
Right Rolandic Operculum	same cluster	4.01	56	−14	10	OP 4 (50%)
Right Rolandic Operculum	same cluster	3.95	60	−4	16	Area 3a (30%)
Right Postcentral Gyrus	124	3.11	44	−30	48	Area 2 (80%)
Right Postcentral Gyrus	same cluster	2.51	40	−40	60	Area 1 (80%)
Right Superior Parietal Lobule	13	2.25	32	−50	60	Area 2 (40%)
Temporal Lobe						
Left Superior Temporal Gyrus	6841 (previous cluster)	6.89	−56	−4	−2	
Right Superior Temporal Gyrus	2454 (previous cluster)	5.69	58	−32	22	IPC (PFcm) (50%)
Right Superior Temporal Gyrus	same cluster	3.99	58	−12	8	TE 1.0 (50%)
Left Middle Temporal Gyrus	17	2.51	−46	−70	8	
Subcortical						
Left Putamen	6841 (previous cluster)	8.13	−24	−2	−6	
Left Thalamus	same cluster	8.08	−20	−16	0	Th−Premotor (33%)
Left Pallidum	same cluster	3.94	−26	−8	−4	
Right Pallidum	2454 (previous cluster)	8.13	26	−4	−2	
Right Putamen	same cluster	3.94	28	8	4	
Right Thalamus	215	8.13	14	−16	0	Th−Premotor (73%)

PFC > Motor Label	Cluster Size	*Z*	Co-ordinate (*x y z*)			Cytoarchitectonic BA (Probability if available)
Cerebellum						
Left Cerebellum	5842	8.13	−34	−62	−40	Lobule VIIa Crus I (58%)
Frontal Lobe						
Left Inferior Frontal Gyrus (p. Triangularis)	1931	8.13	−32	28	0	
Left Inferior Frontal Gyrus (p. Orbitalis)	same cluster	3.96	−44	26	−14	
Left Insula Lobe	same cluster	3.6	−26	26	−4	
Left Inferior Frontal Gyrus (p. Orbitalis)	same cluster	3.35	−54	24	−8	
Left Inferior Frontal Gyrus (p. Triangularis)	same cluster	3.2	−54	28	16	Area 45 (80%)
Left Middle Frontal Gyrus	same cluster	3.17	−36	34	22	
Right Middle Frontal Gyrus	739	6.53	46	34	30	
Right Inferior Frontal Gyrus (p. Triangularis)	same cluster	3.67	52	26	22	
Right Inferior Frontal Gyrus (p. Opercularis)	same cluster	3.66	52	18	34	Area 45 (60%)
Right Inferior Frontal Gyrus (p. Triangularis)	same cluster	3.49	52	28	16	Area 45 (70%)
Right Precentral Gyrus	same cluster	3.06	50	10	32	Area 44 (40%)
Left Superior Medial Gyrus	563	8.13	0	28	40	
Right Superior Medial Gyrus	same cluster	6.96	6	26	44	

TABLE IV. (continued).

PFC > Motor Label	Cluster Size	Z	Co-ordinate (x y z)			Cytoarchitectonic BA (Probability if available)
Right Middle Cingulate Cortex	same cluster	3.94	10	28	38	
Right Insula Lobe	558	8.13	42	22	−10	
Right Inferior Frontal Gyrus (p. Orbitalis)	same cluster	3.94	42	28	−8	
Right Inferior Frontal Gyrus (p. Triangularis)	same cluster	3.2	50	26	2	Area 45 (50%)
Right Middle Frontal Gyrus	111	3.54	32	48	18	
Left Precentral Gyrus	109	3.28	−38	2	58	
Left Middle Frontal Gyrus	same cluster	2.92	−46	6	54	
Right Middle Frontal Gyrus	70	2.31	34	2	62	
Right SMA	20	2.94	8	20	60	
Parietal Lobe						
Left Inferior Parietal Lobule	715	8.13	−38	−50	42	hIP1 (50%)
Left Superior Parietal Lobule	same cluster	5.52	−34	−64	48	SPL (7A) (50%)
Left Inferior Parietal Lobule	same cluster	2.06	−44	−50	56	IPC (PFm) (40%)
Right Angular Gyrus	569	6.31	38	−62	50	
Right Inferior Parietal Lobule	same cluster	4.9	42	−56	50	IPC (PGa) (50%)
Right Superior Parietal Lobule	same cluster	4.82	40	−56	54	SPL (7A) (60%)
Right Inferior Parietal Lobule	same cluster	2.75	52	−46	52	IPC (PFm) (90%)
Right Inferior Parietal Lobule	same cluster	1.99	56	−40	46	IPC (PF) (50%)
Temporal Lobe						
Left Middle Temporal Gyrus	107	3.94	−56	−42	0	
Occipital Lobe						
Right Middle Occipital Gyrus	36	3.45	34	−82	6	
Subcortical						
Right Pallidum	74	2.58	14	4	0	n/a

Cluster size indicates the number of voxels. Cytoarchitectonic and anatomical probabilities were established where possible using the Anatomy toolbox (Eickhoff et al., 2007; Eickhoff et al., 2006; Eickhoff et al., 2005).

Figure 6 illustrates the behavioral domains and paradigm classes that activated cerebellar lobules HV, HVI (Fig. 6a) and HVIIb, HVIII (Fig. 6b) compared with base rate, and differences between these sources (Fig. 6c). Activations within both VOIs were present for action, and action execution studies. However, cerebellar lobules HVIIb and HVIII showed significant greater activation for tasks involved action inhibition and action observation

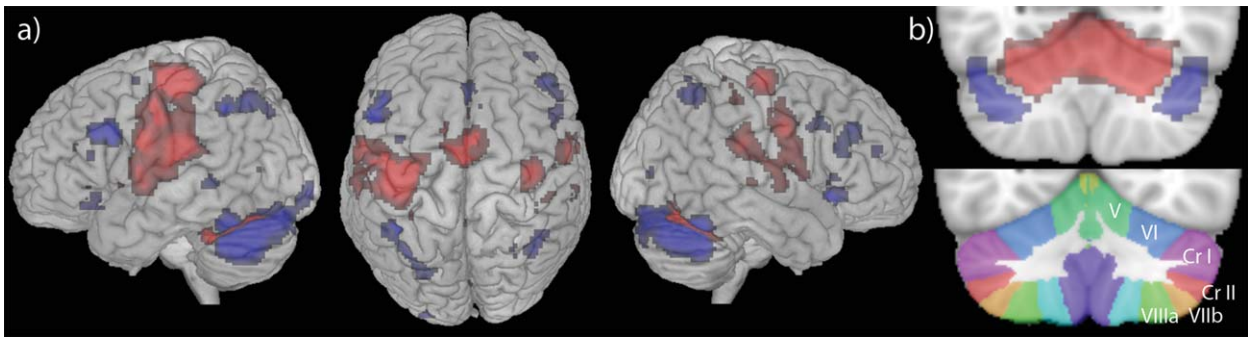

Figure 3.

MACM connectivity differences maps. Red activations show where lobules HV, HVI, HVIIb, HVIII had greater connectivity than lobules Crus I and II. Blue activations show where connectivity was greater for Crus I and II compared with lobules HV, HVI, HVIIb, HVIII. **A**: Shows left hemisphere, top view and right hemisphere activations rendered on ch2better.nii anatomical image. **B**: Shows coronal slices with cerebellar activations along with the same slice of the probabilistic cerebellar atlas [Diedrichsen et al., 2009] for comparison.

TABLE V. Differences in MACM functional connectivity between lobules HV, HVI, and HVIIb, HVIII

Ant motor > Post motor Label	Cluster Size	*Z*	Co-ordinate (*x y z*)			Cytoarchitectonic BA (Probability if available)
Cerebellum						
Left Cerebellum	7119	8.13	−22	−56	−32	lobule HVI (14%)
Frontal Lobe						
Left Postcentral Gyrus	1031	3.9	−52	−10	26	Area 3b (40%)
Left Precentral Gyrus	same cluster	3.3	−38	−8	60	Area 6 (50%)
Left Postcentral Gyrus	same cluster	3.28	−46	−12	30	Area 3a (50%)
Left Postcentral Gyrus	same cluster	2.49	−52	−18	20	OP 1 (40%)
Right SMA	679	3.78	2	−6	56	Area 6 (80%)
Right Postcentral Gyrus	563	3.45	50	−12	32	Area 3b (80%)
RightPrecentral Gyrus	283	3.24	40	−12	54	Area 6 (50%)
Right Postcentral Gyrus	same cluster	2.94	42	−20	50	Area 3b (90%)
Right Insula Lobe	183	2.62	44	10	2	
Left Postcentral Gyrus	14	2.16	−38	−26	46	Area 3a (60%)
Parietal Lobe						
Right SupraMarginal Gyrus	358	2.63	62	−26	26	IPC (PF) (40%)
Right SupraMarginal Gyrus	same cluster	2.55	62	−20	24	IPC (PFop) (30%)
Left Superior Parietal Lobule	58	2.23	−18	−68	46	SPL (7A) (30%)
Temporal Lobe						
Left Superior Temporal Gyrus	64	2.23	−50	−4	−8	
Occipital Lobe						
Left Middle Occipital Gyrus	90	3.2	−32	−90	−6	hOC4v (V4) (40%)
Subcortical						
Left Thalamus	355	3.49	−8	−10	−2	Th−Prefrontal (90%)
Right Thalamus	120	2.56	16	−16	4	Th−Premotor (65%)
Right Thalamus	same cluster	2.51	14	−20	2	Th−Motor (34%)
Right Pallidum	100	2.39	24	−6	6	
Left Putamen	92	2.88	−28	−14	0	

Post motor > Ant motor Label	Cluster Size	*Z*	Co-ordinate (*x y z*)			Cytoarchitectonic BA (Probability if available)
Cerebellum						
Left Cerebellum	1721	8.13	−24	−64	−50	Lobule HVIIIa (70%)
Right Cerebellum	same cluster	4.86	6	−74	−36	Lobule VIIb (46%)
Left Cerebellum	same cluster	3.58	−16	−54	−58	Lobule HVIIIb (85%)
Right Cerebellum	145	4.7	20	−66	−50	Lobule HVIIIa (60%)
Frontal Lobe						
Left Superior Medial Gyrus	370	6.27	−2	20	42	
Left SMA	same cluster	3.22	−8	16	52	
Left Inferior Frontal Gyrus (p. Triangularis)	140	3.45	−38	28	24	
Right Inferior Frontal Gyrus (p. Orbitalis)	87	3.19	36	28	−6	
Left Insula Lobe	41	2.73	−32	20	−6	
Right Middle Cingulate Cortex	12	2.18	4	18	30	
Parietal Lobe						
Left Inferior Parietal Lobule	131	3.09	−44	−44	46	hIP2 (20%)
Subcortical						
Right Pallidum	46	2.11	14	6	−2	n/a
Left Thalamus	37	2.5	−16	−22	14	Th−Parietal (36%)
Left Thalamus	same cluster	2.14	−12	−24	8	Th−Prefrontal (56%)

Cluster size indicates the number of voxels. Cytoarchitectonic and anatomical probabilities were established where possible using the Anatomy toolbox (Eickhoff et al., 2007; Eickhoff et al., 2006; Eickhoff et al., 2005).

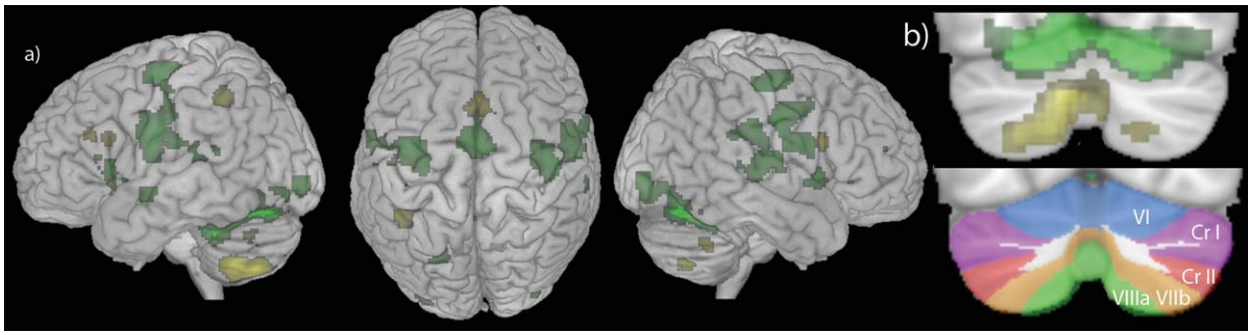

Figure 4.

MACM connectivity differences maps. Green activations show where lobules HV and HVI had greater connectivity than lobules HVIIb and HVIII. Yellow activations show where connectivity was greater for HVIIb and HVIII compared with lobules HV and HVI. **A**: Shows left hemisphere, top view and right hemisphere activations rendered on ch2better.nii anatomical image. **B**: Show coronal slices with cerebellar activations along with the same slice of the probabilistic cerebellar atlas [Diedrichsen et al., 2009] for comparison.

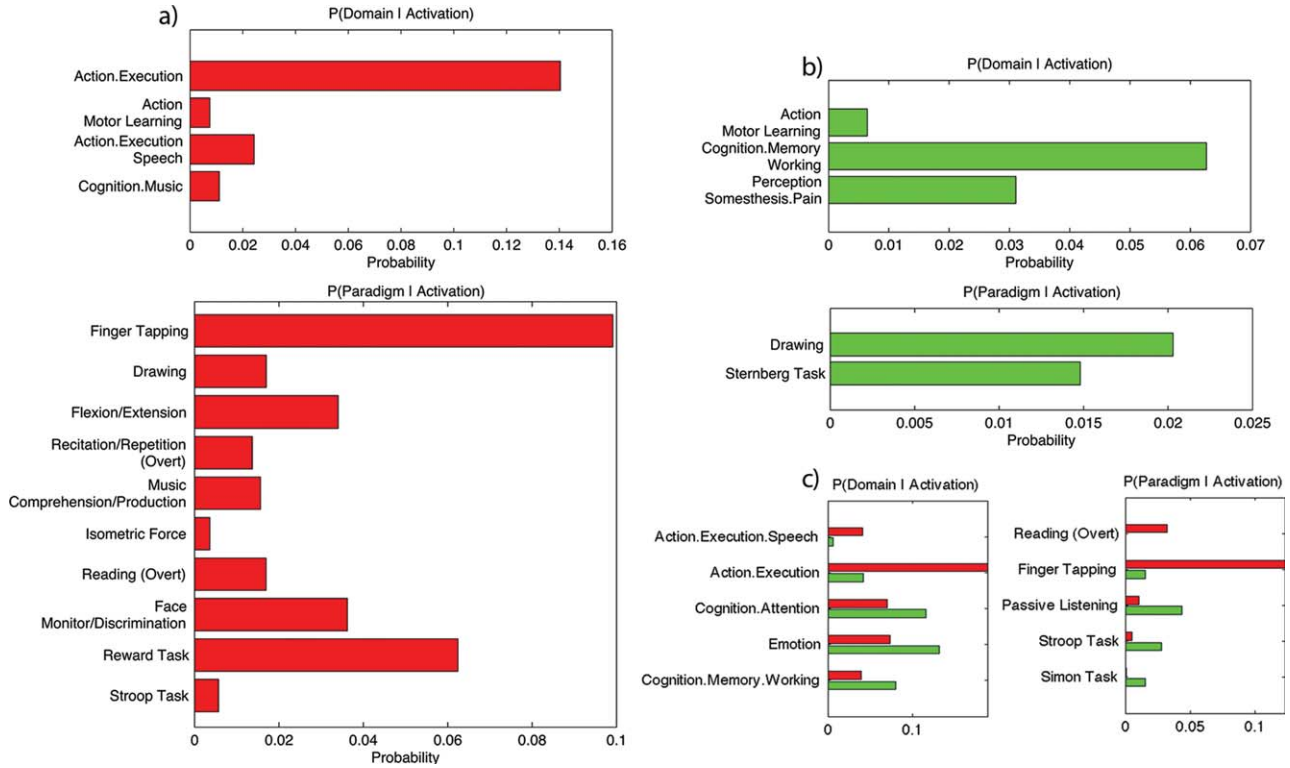

Figure 5.

Functional profiling of cerebellar "motor" (HV, HVI, HVIIb, HVIII) and "prefrontal" (Crus I and Crus II) lobules. Bar plots show significant associations (FDR corrected, $P < 0.05$) of a psychological term (behavioral domains and paradigm classes) from BrainMap meta-data given observed brain activity. Functional profiling was performed as individual motor (**A**) and prefrontal (**B**) masks, and difference analyses (**C**). In all plots the *x*-axis indicates relative probability values, red refers to "motor" cerebellar lobules and green refers to "prefrontal" cerebellar lobules.

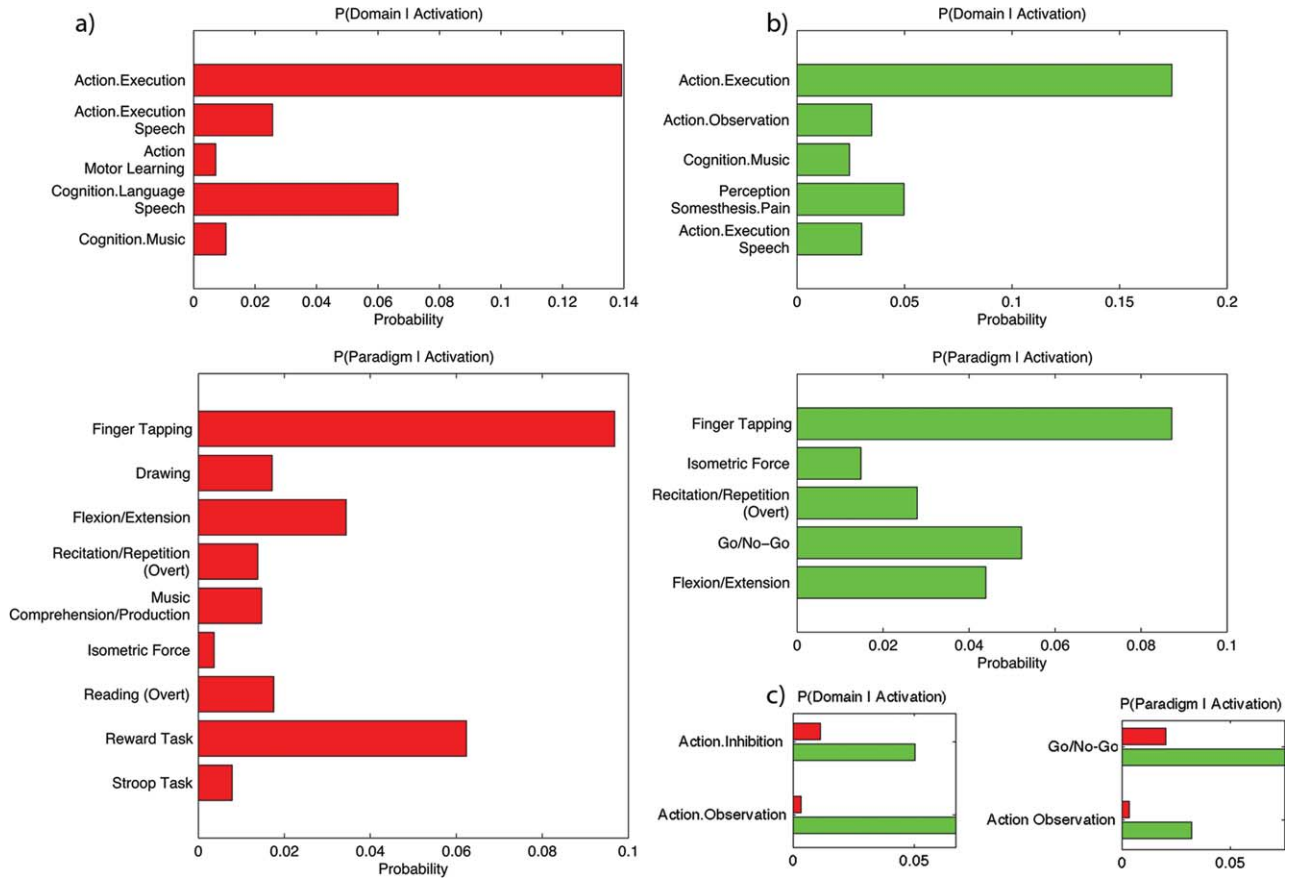

Figure 6.

Functional profiling of cerebellar anterior (HV, HVI) and posterior (HVIIb, HVIII) "motor" lobules. Bar plots show significant associations (FDR corrected, $P < 0.05$) of a psychological term (behavioral domains and paradigm classes) from BrainMap metadata given observed brain activity. Functional profiling was performed as individual anterior (**A**) and posterior (**B**) masks, and difference analyses (**C**). In all plots the *x*-axis indicates relative probability values, red refers to anterior cerebellar "motor" lobules and green refers to posterior cerebellar "motor" lobules.

(Fig. 6c green) compared with anterior motor lobules (Fig. 6c red). The paradigms that drove these differences between anterior and posterior lobules were Go/No-Go tasks and action observation (Fig. 6c green).

DISCUSSION

Studies investigating the anatomy of the cortico-cerebellar system have greatly contributed to the debate surrounding cerebellar contributions to cognition. Connectivity studies in both humans and nonhuman primates suggest that functionally distinct cortico-cerebellar loops exist; one concerned with "sensorimotor" information the other with "associative/non-motor" information [Stoodley, 2012]. This distinction is further supported by functional neuroimaging studies, perhaps most clearly and concisely shown through the use of meta-analytic tools [E et al., 2012; Moulton et al., 2010; Petacchi et al., 2005; Stoodley and Schmahmann, 2009]. However, these aforementioned studies focused solely on activity within the cerebellum and did not investigate cortico-cerebellar connectivity. This study uses MACM to bridge the large gap in the cortico-cerebellar literature between task-independent studies of connectivity and task-dependent functional neuroimaging studies. Our results show that cerebellar lobules HV, HVI, HVIIb, and HVIII had greater coactivation with motor and somatosensory regions compared with lobules Crus I and II which showed greater coactivation with prefrontal and parietal regions. These separate coactivation profiles were driven by distinct behavioral domains as well. Regions that coactivated with Crus I and II were primarily driven by emotion and cognitive tasks, while regions that coactivated with HV, HVI, HVIIb, and HVIII were driven by motor tasks.

Distinct "Associative" and "Motor" Cortico-Cerebellar Circuits

One key feature of this study is that connectivity patterns established using task-independent methods such as tracer studies, diffusion tractography, or resting fMRI, were replicated when using task-dependent data. As repeatedly seen in connectivity studies using humans [Buckner et al., 2011; Krienen and Buckner, 2009; O'Reilly et al., 2010] and nonhuman primates [Kelly and Strick, 2003] we found that lobules Crus I and II were coactivated with prefrontal and parietal cortices, whilst lobules HV, HVI, HVIIb, and HVIII were coactivated with the pre- and postcentral gyrus (see Fig. 3). It is possible that by collapsing across lobules Crus I and II, or HV and HVI, we are introducing additional heterogeneity into the analyses and that lobules within each mask might have distinct roles to play in either motor or cognitive processes. For this reason we have provided additional analyses of individual lobules in Supporting Information. However, we would argue that analyses combining these cerebellar lobules are relevant given that they (1) conform with previous anatomical and functional connectivity studies [Kelly and Strick, 2003; O'Reilly et al., 2010], (2) conform with studies showing lobule specific evolutionary expansion [Balsters et al., 2010] and most importantly, (3) the paradigm class information extracted from these masks shows a clear distinction between cognitive paradigms (Crus I and II) and motor paradigms (HV, HVI, HVIIb, and HVIII) which were found to evoke activations in these masks. Figure 2 shows a large degree of overlap between coactivation patterns from Crus I and II VOIs, and coactivation patterns from HV, HVI, HVIIb, HVIII VOIs (see Fig. 2e). However, we believe this is because the majority of cognitive paradigms also include a motor response to establish whether the participant has performed the task correctly. This is a particularly important issue for cerebellar studies where it is important to disambiguate cognitive processes from subsequent motor processes [see Balsters and Ramnani, 2008, 2011; Balsters et al., 2013 for examples using temporal jittering]. FMRI studies of cognitive control typically include a motor response directly after a cue and the "cognitive subtraction" approach is then used to remove common motor processes and isolate distinct cognitive processes. Given the large number of studies included in the generation of these MACMs (~52,000 foci), it is not possible to assess how many of these studies have used a control condition or quality of the control condition used. Rather than constrain the analyses to particular types of contrasts we performed the analyses in a purely data-driven fashion. By contrasting the maps generated using MACM we can clearly highlight the unique connectivity patterns of these functionally distinct (as confirmed by the paradigm class information) sets of cerebellar lobules. Similar to a standard fMRI study, comparing Crus I and II coactivation patterns with respect to HV, HVI, HVIIb, and HVIII coactivations patterns clearly highlights the distinction between prefrontal-parietal-cerebellar circuits and motor-cerebellar circuits. This distinction was also apparent when analyzing behavioral domain and paradigm class metadata. Studies using cognitive and emotional tasks activated Crus I and II, while studies using motor tasks, specifically action execution, activated HV, HVI, HVIIb, and HVIII. Given differences in the MACM coactivation patterns, and differences in the tasks driving these cortico-cerebellar circuits, these results further suggest that independent cortico-cerebellar circuits contribute to both cognitive and motor control.

Middleton and Strick [2000, 2001] originally proposed that the cortico-cerebellar system was arranged as a collection of independent loops. The results of this study are in concert with this idea; however, it is important to state that even though separate cerebellar lobules were activated by different tasks, this does not mean that distinct regions of the cerebellum are performing different computations. Passingham et al. [2002] states that in order to understand the functions of a cortical region we must investigate its extrinsic connectivity and its intrinsic anatomical features. One of the most distinctive features of the cerebellar cortex is its uniform cellular structure [Eccles et al., 1967]. This uniformity conveys an important functional feature, namely that the cerebellar cortex performs the same process, or series of processes, regardless of whether the cortical input arrives from highly abstract/cognitive regions in the prefrontal cortex, or regions of the primary motor cortex concerned with the specific dynamics of movement. In the present study we find activations in the cerebellar cortex were significantly evoked by Action (execution, motor learning, observation), Cognition (language, music, working memory, attention), and Perception. This is consistent with previous meta-analyses that have also shown the cerebellum is active during a wide array of sensory, motor, and higher cognitive processes [E et al., 2012; Moulton et al., 2010; Petacchi et al., 2005; Stoodley and Schmahmann, 2009]. Even though the current study and others suggest that distinct regions of the cerebellum are involved in processing different behavioral domains, we do not suggest that the role of the cerebellum within these independent cortico-cerebellar circuits differs. Rather, we would agree with the theories proposed by Kawato and Wolpert [Kawato and Wolpert, 1998; Wolpert et al., 1998] as well as Ramnani [2006] that the role of the cerebellar cortex is to automate information processes within cortical territories, regardless of whether that involves automating motor control processes in the primary motor cortex or working memory processes within the prefrontal cortex. For example, Imamizu et al. [2003, 2000] have demonstrated using fMRI that cerebellar lobules HV and HVI reduce in BOLD activity in a manner that conforms to control theoretic models of cerebellar function during the acquisition of a motor skill. Recently, Balsters and Ramnani [2011] extended these ideas to investigate more abstract information processing. While Imamizu et al. [2003, 2000] showed that the acquisition of

motor skills lead to cerebellar plastic changes within cerebellar lobules HV and HVI, Balsters and Ramnani [2011] found that the automation of first-order rules lead to similar cerebellar plastic changes within Crus I, a region of the cerebellum repeatedly shown to be interconnected with the prefrontal cortex. Although this study demonstrates that cortico-cerebellar circuits contribute to distinct behavioral domains, we would maintain that the role of the cerebellum within these circuits is constant, i.e. aiding the automation of cortical processing.

Anatomical and Functional Differences Between Anterior (HV, HVI) and Posterior (HVIIb, HVIII) Cerebellar "Motor" Lobules

Studies of both anatomy and function have led to the proposal that dual routes exist within the cortical motor system [Hoshi and Tanji, 2007; Passingham and Toni, 2001; Rathelot and Strick, 2009]. Studies of the cytoarchitectonic properties of primary motor cortex (BA 4) show a separation between anterior and posterior regions [areas 4a and 4p respectively; Geyer et al., 1996]. This dichotomy was further supported by Rathelot and Strick [2009] who subdivided the precentral gyrus into "old" and "new" M1 based on the presence of cortico-motoneuronal (CM) cells. CM cells within the caudal aspect of the precentral gyrus (putatively area 4p) allow signals from "new" M1 to bypass spinal cord mechanisms and output more complex motor behaviors. Phylo- and optogenetic studies suggest that this region has been "added" over the course of evolution, and is not present in all mammals [Nudo and Masterton, 1988]. Balsters et al. [2010] also demonstrated differences in the evolution of cerebellar lobules by showing that cerebellar lobules HVIIb and HVIIIa had increased in proportional volume in humans compared to nonhuman primates (capuchins and chimpanzees), whilst cerebellar lobules HV and HVI showed a significant decrease in proportional volume in humans compared with nonhuman primates. If evolutionary pressures act on complete functional systems rather than on individual brain areas [Streidter, 2005] then one might predict that posterior cerebellar lobules would show greater connectivity with "new" M1, whilst anterior cerebellar motor lobules would show greater connectivity with "old" M1. This hypothesis was not supported by our results, which showed that cerebellar lobules HV and HVI had greater connectivity with the precentral gyrus overlapping with both areas 4a and 4p compared to cerebellar lobules HVIIb and HVIII. This would suggest that the evolutionary expansion of cerebellar lobules HVIIb and HVIII in humans is not likely to be related to the presence of CM cells and the differentiation between 4a and 4p. On the basis of the anatomical tracing studies of Kelly and Strick [2003], we have assigned lobules HVIIB and HVIII as "motor" lobules. However, these lobules may in fact contribute to prefrontal/cognitive processes. Cerebellar lobules HVIIb and HVIII showed greater connectivity with the superior medial gyrus (putatively Pre-SMA), bilateral inferior frontal gyrus, and the left inferior parietal lobule. The paradigms found to evoke these connectivity differences were action observation and inhibition. Studies of both action inhibition and third person learning have often reported activations within the superior medial gyrus and cingulate cortex [Apps et al., 2012, 2013; Chambers et al., 2009]. It may thus be argued that cerebellar lobules HV and HVI have greater connectivity with the primary motor cortex and play a greater role in motor learning, whilst cerebellar lobules HVIIb and HVIII have increased connectivity with the superior medial gyrus and thus may have an increased role in observational learning, possibly related to the presence of mirror neurons [Cattaneo and Rizzolatti, 2009]. One caveat of this analysis is that the number of experiments and foci contributing to anterior motor lobules is much higher than the number contributing to the posterior cerebellar lobules. Restrictions of the field of view in fMRI and default preprocessing settings in some neuroimaging packages mean that the posterior lobules of the cerebellum are often excluded from analysis and as such may be under-represented in these analyses. Although the exact functional distinction between these cerebellar lobules remains unclear, the use of MACM has helped us to refute potential hypotheses and develop novel hypotheses that will require further exploration, i.e., the possible distinction between action execution and observational learning within anterior and posterior cerebellar "motor" lobules.

Functional vs. Anatomical Cerebellar Parcellation

This study, like many others, used anatomical VOIs to investigate connectivity. There are two main reasons for this; (1) this approach is in keeping with the majority of cerebellar connectivity studies (both non-human primate tracer studies and resting state fMRI studies) which have discussed their results in terms of lobular cerebellar anatomy, and (2) a probabilistic atlas based on the lobular anatomy of the cerebellar cortex is available to facilitate this type of analysis [Diedrichsen et al., 2009]. However, the cerebellum can also be categorised based on climbing fiber inputs originating from the inferior olive [Pijpers et al., 2005; Ruigrok, 2011; Voogd, 2012]. Studies investigating cortico-ponto-cerebellar-thalamic loops have described an anterior–posterior cerebellar functional topography, but studies of olivo-cerebellar connectivity have demonstrated a medial-lateral functional topography within the cerebellum. Unfortunately it is not currently possible to investigate this olivo-cerebellar functional organisation using MRI, but resting state connectivity studies have begun using hierarchical clustering as an alternative to anatomical VOIs. Both Buckner et al. [2011] and Bernard et al. [2012] recently investigated cortico-

cerebellar connectivity using a hierarchical clustering approach. The results of both analyses suggest that anatomical parcellations of the cerebellar cortex may be a rather crude approach that does not pick up functional sub-regions within cerebellar lobules. For example, both Buckner et al. [2011] and Bernard et al. [2012] show that Crus I contains 2–4 functional subdivisions. However, one broad criticism of hierarchical clustering approaches is that there is no gold-standard in choosing the correct or even just the optimal number of clusters. This can be seen when one compares Buckner et al [2011] (either 7 or 17 clusters) with Bernard et al. [2012] (20 clusters). The clustering algorithm of Bernard et al. [2012] separated lobules HV and HVI from lobules HVIIb and HVIII as functionally distinct units whilst neither of the solutions provided by Buckner et al. [2011] does. Although it is likely that these studies are more sensitive to functional subdivisions within the cerebellum there is still a great deal of uncertainty regarding this approach. An important extension of the present study would be to apply hierarchical clustering approaches to this task-dependent dataset. It is likely that the clustering achieved using task-dependent information compared to task-free fluctuations will be more informative and could help to refine our understanding of functional cortico-cerebellar differences. It would also be of interest to investigate MACM differences between cerebellar vermis and hemisphere. The cerebellar vermis has been linked to a wide array of behaviors such as posture and gait, eye movement, and emotional processing [Schmahmann, 1997]. Unfortunately, the size of the cerebellar vermis is very small (<5% of the total cerebellar grey matter; Diedrichsen et al., 2009), and the relative sizes of vermal lobules range from 1.67% (lobule VI) to 0.05% (Crus I) total grey matter. Given the limited size of the cerebellar vermis as a whole, as well as the vermal components of specific lobules, it was not possible to extract enough activation foci within these regions to perform a reliable MACM analysis.

CONCLUSIONS AND OUTLOOK

This study provides the first evidence that cortico-cerebellar circuits established using task-independent methods are also present using task-dependent data. MACM also provided behavioral meta-data demonstrating that these independent cortico-cerebellar circuits are driven by distinct tasks. While this is important for developing our understanding of cerebellar information processing it is also important for understanding the consequences of cerebellar damage in different disease states. Reetz et al. [2012] used VBM to identify differences in cerebellar grey matter volume in a population with spinocerebellar ataxia 17 (SCA 17) compared with matched controls. Using cerebellar group differences as VOIs it was then possible to investigate task-independent connectivity using resting state fMRI and task-dependent connectivity using MACM in a much larger sample of healthy controls. This approach highlights the behavioral and connectivity profiles of these affected regions in healthy individuals and then allows one to infer the likely consequences of damage to these regions. The results of Reetz et al. [2012] showed that both cognitive and motor cortico-cerebellar circuits were damaged, explaining the brunt of motor deficits but also the broad spectrum of neuropsychiatric deficits seen in SCA17. The present study and the study of Reetz et al. [2012] highlight the potential of MACM both as a method for probing the functions of neuroanatomical circuits in healthy individuals, and as a tool to investigate the clinical relevance of cerebellar damage.

REFERENCES

Apps MA, Balsters JH, Ramnani N (2012): The anterior cingulate cortex: Monitoring the outcomes of others' decisions. Soc Neurosci 7:424–435.

Apps MA, Green R, Ramnani N (2013): Reinforcement learning signals in the anterior cingulate cortex code for others' false beliefs. Neuroimage 64:1–9.

Badre D, D'Esposito M (2009): Is the rostro-caudal axis of the frontal lobe hierarchical? Nat Rev Neurosci 10:659–669.

Balsters JH, Cussans E, Diedrichsen J, Phillips KA, Preuss TM, Rilling JK, Ramnani N (2010): Evolution of the cerebellar cortex: The selective expansion of prefrontal-projecting cerebellar lobules. Neuroimage 49:2045–2052.

Balsters JH, Ramnani N (2008): Symbolic representations of action in the human cerebellum. Neuroimage 43:388–398.

Balsters JH, Ramnani N (2011): Cerebellar plasticity and the automation of first-order rules. J Neurosci 31:2305–2312.

Balsters JH, Whelan CD, Robertson IH, Ramnani N (2013): Cerebellum and cognition: Evidence for the encoding of higher order rules. Cereb Cortex 23:1433–1443.

Bernard JA, Seidler RD, Hassevoort KM, Benson BL, Welsh RC, Wiggins JL, Jaeggi SM, Buschkuehl M, Monk CS, Jonides J, et al. (2012): Resting state cortico-cerebellar functional connectivity networks: a comparison of anatomical and self-organizing map approaches. Front Neuroanat 6:31.

Buckner RL, Krienen FM, Castellanos A, Diaz JC, Yeo BT (2011): The organization of the human cerebellum estimated by intrinsic functional connectivity. J Neurophysiol 106:2322–2345.

Caspers S, Zilles K, Laird AR, Eickhoff SB (2010): ALE meta-analysis of action observation and imitation in the human brain. Neuroimage 50:1148–1167.

Cattaneo L, Rizzolatti G (2009): The mirror neuron system. Arch Neurol 66:557–560.

Chambers CD, Garavan H, Bellgrove MA (2009): Insights into the neural basis of response inhibition from cognitive and clinical neuroscience. Neurosci Biobehav Rev 33:631–646.

Cieslik EC, Zilles K, Caspers S, Roski C, Kellermann TS, Jakobs O, Langner R, Laird AR, Fox PT, Eickhoff SB (2012): Is there "One" DLPFC in cognitive action control? Evidence for heterogeneity from co-activation-based parcellation. Cereb Cortex.

Crick FC, Koch C (2005): What is the function of the claustrum? Philos Trans R Soc Lond B Biol Sci 360:1271–1279.

Diedrichsen J (2006): A spatially unbiased atlas template of the human cerebellum. Neuroimage 33:127–138.

Diedrichsen J, Balsters JH, Flavell J, Cussans E, Ramnani N (2009): A probabilistic MR atlas of the human cerebellum. Neuroimage 46:39–46.

E KH, Chen SH, Ho MH, Desmond JE (2012): A meta-analysis of cerebellar contributions to higher cognition from PET and fMRI studies. Hum Brain Mapp.

Eccles JC, Ito M, Szentagothai J (1967): The Cerebellum as a Neuronal Machine. New York: Springer-Verlag.

Eickhoff SB, Bzdok D, Laird AR, Kurth F, Fox PT (2012): Activation likelihood estimation meta-analysis revisited. Neuroimage 59:2349–2361.

Eickhoff SB, Bzdok D, Laird AR, Roski C, Caspers S, Zilles K, Fox PT (2011): Co-activation patterns distinguish cortical modules, their connectivity and functional differentiation. Neuroimage 57:938–949.

Eickhoff SB, Grefkes C (2011): Approaches for the integrated analysis of structure, function and connectivity of the human brain. Clin EEG Neurosci 42:107–121.

Eickhoff SB, Jbabdi S, Caspers S, Laird AR, Fox PT, Zilles K, Behrens TE (2010): Anatomical and functional connectivity of cytoarchitectonic areas within the human parietal operculum. J Neurosci 30:6409–6421.

Eickhoff SB, Laird AR, Grefkes C, Wang LE, Zilles K, Fox PT (2009): Coordinate-based activation likelihood estimation meta-analysis of neuroimaging data: A random-effects approach based on empirical estimates of spatial uncertainty. Hum Brain Mapp 30:2907–2926.

Eickhoff SB, Paus T, Caspers S, Grosbras MH, Evans AC, Zilles K, Amunts K (2007): Assignment of functional activations to probabilistic cytoarchitectonic areas revisited. Neuroimage 36: 511–521.

Eickhoff SB, Schleicher A, Zilles K, Amunts K (2006): The human parietal operculum. I. Cytoarchitectonic mapping of subdivisions. Cereb Cortex 16:254–267.

Eickhoff SB, Stephan KE, Mohlberg H, Grefkes C, Fink GR, Amunts K, Zilles K (2005): A new SPM toolbox for combining probabilistic cytoarchitectonic maps and functional imaging data. Neuroimage 25:1325–1335.

Fox PT, Laird AR, Fox SP, Fox PM, Uecker AM, Crank M, Koenig SF, Lancaster JL (2005): BrainMap taxonomy of experimental design: Description and evaluation. Hum Brain Mapp 25:185–198.

Fox PT, Lancaster JL (2002): Opinion: Mapping context and content: The BrainMap model. Nat Rev Neurosci 3:319–321.

Geyer S, Ledberg A, Schleicher A, Kinomura S, Schormann T, Burgel U, Klingberg T, Larsson J, Zilles K, Roland PE (1996): Two different areas within the primary motor cortex of man. Nature 382:805–807.

Habas C, Kamdar N, Nguyen D, Prater K, Beckmann CF, Menon V, Greicius MD (2009): Distinct cerebellar contributions to intrinsic connectivity networks. J Neurosci 29:8586–8594.

Hoshi E, Tanji J (2007): Distinctions between dorsal and ventral premotor areas: Anatomical connectivity and functional properties. Curr Opin Neurobiol 17:234–242.

Imamizu H, Kuroda T, Miyauchi S, Yoshioka T, Kawato M (2003): Modular organization of internal models of tools in the human cerebellum. Proc Natl Acad Sci USA 100:5461–5466.

Imamizu H, Miyauchi S, Tamada T, Sasaki Y, Takino R, Putz B, Yoshioka T, Kawato M (2000): Human cerebellar activity reflecting an acquired internal model of a new tool. Nature 403:192–195.

Kawato M, Wolpert D (1998): Internal models for motor control. Novartis Found Symp 218:291–304; discussion 304–307.

Kelly RM, Strick PL (2003): Cerebellar loops with motor cortex and prefrontal cortex of a nonhuman primate. J Neurosci 23: 8432–8444.

Krienen FM, Buckner RL (2009): Segregated fronto-cerebellar circuits revealed by intrinsic functional connectivity. Cereb Cortex 19:2485–2497.

Laird AR, Eickhoff SB, Fox PM, Uecker AM, Ray KL, Saenz JJ, Jr., McKay DR, Bzdok D, Laird RW, Robinson JL, et al. (2011): The BrainMap strategy for standardization, sharing, and meta-analysis of neuroimaging data. BMC Res Notes 4:349.

Laird AR, Eickhoff SB, Kurth F, Fox PM, Uecker AM, Turner JA, Robinson JL, Lancaster JL, Fox PT (2009a): ALE meta-analysis workflows via the brainmap database: Progress towards a probabilistic functional brain Atlas. Front Neuroinform 3:23.

Laird AR, Eickhoff SB, Li K, Robin DA, Glahn DC, Fox PT (2009b): Investigating the functional heterogeneity of the default mode network using coordinate-based meta-analytic modeling. J Neurosci 29:14496–14505.

Laird AR, Lancaster JL, Fox PT (2005): BrainMap: the social evolution of a human brain mapping database. Neuroinformatics 3: 65–78.

Lancaster JL, Tordesillas-Gutierrez D, Martinez M, Salinas F, Evans A, Zilles K, Mazziotta JC, Fox PT (2007): Bias between MNI and Talairach coordinates analyzed using the ICBM-152 brain template. Hum Brain Mapp 28:1194–1205.

Larsell O, Jansen O (1972): The Comparative Anatomy and Histology of the Cerebellum: The Human Cerebellum, Cerebellar Connections and Cerebellar Cortex. Minneapolis: University of Minnesota Press.

Middleton FA, Strick PL (2000): Basal ganglia and cerebellar loops: Motor and cognitive circuits. Brain Res Brain Res Rev 31(2-3):236–250.

Middleton FA, Strick PL (2001): Cerebellar projections to the prefrontal cortex of the primate. J Neurosci 21:700–712.

Moulton EA, Schmahmann JD, Becerra L, Borsook D (2010): The cerebellum and pain: Passive integrator or active participator? Brain Res Rev 65:14–27.

Nichols T, Brett M, Andersson J, Wager T, Poline JB (2005): Valid conjunction inference with the minimum statistic. Neuroimage 25:653–660.

Nickl-Jockschat T, Schneider F, Pagel AD, Laird AR, Fox PT, Eickhoff SB (2011): Progressive pathology is functionally linked to the domains of language and emotion: Meta-analysis of brain structure changes in schizophrenia patients. Eur Arch Psychiatry Clin Neurosci 261 (Suppl 2):S166–S171.

Nudo RJ, Masterton RB (1988): Descending pathways to the spinal cord: A comparative study of 22 mammals. J Comp Neurol 277:53–79.

O'Reilly JX, Beckmann CF, Tomassini V, Ramnani N, Johansen-Berg H (2010): Distinct and overlapping functional zones in the cerebellum defined by resting state functional connectivity. Cereb Cortex 20:953–965.

Passingham RE, Stephan KE, Kotter R (2002): The anatomical basis of functional localization in the cortex. Nat Rev Neurosci 3:606–616.

Passingham RE, Toni I (2001): Contrasting the dorsal and ventral visual systems: Guidance of movement versus decision making. Neuroimage 14(1 Part 2):S125–S131.

Petacchi A, Laird AR, Fox PT, Bower JM (2005): Cerebellum and auditory function: An ALE meta-analysis of functional neuroimaging studies. Hum Brain Mapp 25:118–128.

Pijpers A, Voogd J, Ruigrok TJ (2005): Topography of olivo-cortico-nuclear modules in the intermediate cerebellum of the rat. J Comp Neurol 492:193–213.

Ramnani N (2006): The primate cortico-cerebellar system: Anatomy and function. Nat Rev Neurosci 7:511–522.

Ramnani N (2011): Frontal lobe and posterior parietal contributions to the cortico-cerebellar system. Cerebellum.

Ramnani N, Behrens TE, Johansen-Berg H, Richter MC, Pinsk MA, Andersson JL, Rudebeck P, Ciccarelli O, Richter W, Thompson AJ, et al. (2006): The evolution of prefrontal inputs to the cortico-pontine system: Diffusion imaging evidence from Macaque monkeys and humans. Cereb Cortex 16:811–818.

Rathelot JA, Strick PL (2009): Subdivisions of primary motor cortex based on cortico-motoneuronal cells. Proc Natl Acad Sci USA 106:918–923.

Reetz K, Dogan I, Rolfs A, Binkofski F, Schulz JB, Laird AR, Fox PT, Eickhoff SB (2012): Investigating function and connectivity of morphometric findings—Exemplified on cerebellar atrophy in spinocerebellar ataxia 17 (SCA17). Neuroimage 62:1354–1366.

Robinson JL, Laird AR, Glahn DC, Blangero J, Sanghera MK, Pessoa L, Fox PM, Uecker A, Friehs G, Young KA, et al. (2012): The functional connectivity of the human caudate: An application of meta-analytic connectivity modeling with behavioral filtering. Neuroimage 60:117–129.

Robinson JL, Laird AR, Glahn DC, Lovallo WR, Fox PT (2010): Meta-analytic connectivity modeling: Delineating the functional connectivity of the human amygdala. Hum Brain Mapp 31:173–184.

Rottschy C, Langner R, Dogan I, Reetz K, Laird AR, Schulz JB, Fox PT, Eickhoff SB (2012): Modelling neural correlates of working memory: A coordinate-based meta-analysis. Neuroimage 60:830–846.

Ruigrok TJ (2011): Ins and outs of cerebellar modules. Cerebellum 10:464–474.

Schmahmann JD (1997): Rediscovery of an early concept. Int Rev Neurobiol 41:3–27.

Schmahmann JD, Pandya DN (1997): Anatomic organization of the basilar pontine projections from prefrontal cortices in rhesus monkey. J Neurosci 17:438–458.

Stoodley CJ (2012): The cerebellum and cognition: Evidence from functional imaging studies. Cerebellum 11:352–365.

Stoodley CJ, Schmahmann JD (2009): Functional topography in the human cerebellum: A meta-analysis of neuroimaging studies. Neuroimage 44:489–501.

Streidter GF (2005): Concerted and Mosaic Evolution. Principles of Brain Evolution. Sunderland, MA: Sinauer Associates.

Strick PL, Dum RP, Fiez JA (2009): Cerebellum and nonmotor function. Annu Rev Neurosci 32:413–434.

Turkeltaub PE, Eickhoff SB, Laird AR, Fox M, Wiener M, Fox P (2012): Minimizing within-experiment and within-group effects in Activation Likelihood Estimation meta-analyses. Hum Brain Mapp 33:1–13.

Voogd J (2012): A note on the definition and the development of cerebellar Purkinje cell zones. Cerebellum 11:422–425.

Walker AE (1940): A cytoarchitectural study of the prefrontal area of the macaque monkey. J Comp Neurol 73:59–86.

Wolpert DM, Miall C, Kawato M (1998): Internal models in the cerebellum. Trends Cogn Sci 2:338–347.